© <2017>. This manuscript version is made available under the CC-BY-NC-ND 4.0 license

http://creativecommons.org/licenses/by-nc-nd/4.0/

Accepted Manuscript

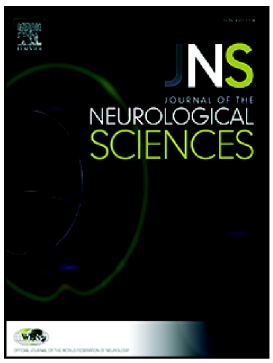

Global brain atrophy and metabolic dysfunction in LGI1 encephalitis: A prospective multimodal MRI study

Monika Szots, Morten Blaabjerg, Gergely Orsi, Pernille Iversen, Daniel Kondziella, Camilla G. Madsen, Ellen Garde, Peter Magnusson, Peter Barsi, Ferenc Nagy, Hartwig R. Siebner, Zsolt Illes

PII: S0022-510X(17)30190-9
DOI: doi: 10.1016/j.jns.2017.03.020
Reference: JNS 15220

To appear in: *Journal of the Neurological Sciences*

Received date: 3 January 2017
Revised date: 19 February 2017
Accepted date: 14 March 2017

Please cite this article as: Monika Szots, Morten Blaabjerg, Gergely Orsi, Pernille Iversen, Daniel Kondziella, Camilla G. Madsen, Ellen Garde, Peter Magnusson, Peter Barsi, Ferenc Nagy, Hartwig R. Siebner, Zsolt Illes , Global brain atrophy and metabolic dysfunction in LGI1 encephalitis: A prospective multimodal MRI study. The address for the corresponding author was captured as affiliation for all authors. Please check if appropriate. Jns(2017), doi: 10.1016/j.jns.2017.03.020

This is a PDF file of an unedited manuscript that has been accepted for publication. As a service to our customers we are providing this early version of the manuscript. The manuscript will undergo copyediting, typesetting, and review of the resulting proof before it is published in its final form. Please note that during the production process errors may be discovered which could affect the content, and all legal disclaimers that apply to the journal pertain.

ACCEPTED MANUSCRIPT

Global brain atrophy and metabolic dysfunction in LGI1 encephalitis: a prospective multimodal MRI study

Monika Szots[a], Morten Blaabjerg[b,c], Gergely Orsi[d,e], Pernille Iversen[f,g], Daniel Kondziella[h], Camilla G Madsen[f], Ellen Garde[f,i], Peter Magnusson[f], Peter Barsi[j], Ferenc Nagy[a], Hartwig R. Siebner[f,k] Zsolt Illes[b,c,*]

[a]Department of Neurology, Mor Kaposi Teaching Hospital, Kaposvar, Hungary

[b]Department of Neurology, Odense University Hospital, Odense, Denmark

[c]Department of Clinical Research, University of Southern Denmark, Odense, Denmark

[d]MTA-PTE Clinical Neuroscience MR Research Group, Pecs, Hungary

[e]Department of Neurosurgery, Clinical Centre, University of Pecs, Pecs, Hungary

[f]Danish Research Centre for Magnetic Resonance, Centre for Functional and Diagnostic Imaging and Research, Copenhagen University Hospital Hvidovre, Hvidovre, Denmark

[g]CHIP, Department of Infectious Diseases, Rigshospitalet, Copenhagen University Hospital, Copenhagen, Denmark

[h]Department of Neurology, Rigshospitalet, Copenhagen University Hospital, Copenhagen, Denmark

[i]Department of Public Health, Copenhagen University, Copenhagen, Denmark

[j]MR Research Center, Semmelweis University, Budapest, Hungary

[k]Department of Neurology, Copenhagen University Hospital Bispebjerg, Copenhagen, Denmark

[*]**Correspondance:** Zsolt Illes, Department of Neurology, Odense University Hospital, Sdr. Boulevard 29, 5000 Odense C, email: zsolt.illes@rsyd.dk, Denmark, Tel: +45 6541-5332, Fax: +45 6613-8622

ACCEPTED MANUSCRIPT

ACCEPTED MANUSCRIPT

ABSTRACT

Background: Chronic cognitive deficits are frequent in leucin-rich glioma-inactivated 1 protein (LGI1) encephalitis. We examined structural and metabolic brain abnormalities following LGI1 encephalitis and correlated findings with acute and follow-up clinical outcomes.

Methods: Nine patients underwent prospective multimodal 3 Tesla MRI 33.1±18 months after disease onset, including automated volumetry, diffusion tensor imaging (DTI) and magnetic resonance spectroscopy (MRS). Data were compared to 9 age- and sex-matched healthy controls.

Results: Although extratemporal lesions were not present on MRI in the acute stage, tract-based spatial statistics analyses of DTI during follow-up showed widespread changes in the cerebral and cerebellar white matter (WM), most prominent in the anterior parts of the corona radiata, capsula interna and corpus callosum. MRS revealed lower glutamine/glutamate WM levels compared to controls. Higher cerebellar grey matter volume was associated with better function at disease onset (measured by the modified Rankin Scale), and higher putaminal volume was associated with better cognition by Addenbrooke's Cognitive Examination test at 23.4±7.6 months.

Conclusions: Poor clinical outcome following LGI1 encephalitis is associated with global brain atrophy and disintegration of white matter tracts. The pathological changes affect not only temporomesial structures but also frontal lobes and the cerebellum.

Key words: anti-LGI1 antibody, limbic encephalitis, MR-spectroscopy, volumetry, diffusion tensor imaging, cognition

ACCEPTED MANUSCRIPT

ACCEPTED MANUSCRIPT

1. INTRODUCTION

Antibodies against the LGI1 protein of the voltage-gated potassium channel (VGKC) complex result in subacute limbic encephalitis (LE) [1]. While patients with early immunotherapy may have a good prognosis [2,3], cognitive deficit develop in most [4,5]. Structural magnetic resonance imaging (MRI) showed extratemporal T2 hyperintensities in the early phase with faciobrachial (dys)tonic seizures (FBDS) and reduced volume of the whole brain one year after FBDS [6-10]. Glucose metabolism is also abnormal in areas outside of the limbic structures [8,11-13]. Although these data point to global structural and metabolic alterations, no study examined metabolic changes several years after LGI1 encephalitis. Only a single very recent study used follow-up MRI to examine chronic global and regional brain changes and its correlation with memory [14]. The correlation between prospectively obtained MRI/clinical outcomes and clinical/neuroimaging characteristics in the acute phase is not known either.

Therefore, here we examined (i) MRI alterations in the acute stage of LGI1 encephalitis; (ii) evaluated MRI outcomes 33.1±18 months after disease onset by prospectively planned multi-modal MRI; and (iii) correlated MRI outcomes with functional outcomes during the early and later stages of the disease.

ACCEPTED MANUSCRIPT

ACCEPTED MANUSCRIPT

2. MATERIAL AND METHODS

2.1 Participants

Nine patients (4 females, age at onset 59.9±14.5), diagnosed with LGI1 LE participated in this study (**Table 1**). The patients were retrospectively identified in our clinical databases over 53 months (Februar 2009 to July 2013). LGI1-antibodies were present in the serum, and with one exception in the cerebrospinal fluid (CSF) (IIFT Autoimmune Mosaic 1, Euroimmun, Lübeck, Germany). Three patients were treated in Hungary and six patients were treated in Denmark. Nine Hungarian age- and sex-matched healthy volunteers (mean age: 62.00±13.4 years) were included, matching criterion of age was ± 3 years. Clinical information was retrospectively obtained from medical reports and from interviews with the individual patient's neurologist. Mini-Mental State Examination (MMSE) and modified Rankin scale (mRS) were regularly controlled. We performed correlation analysis with MMSE and mRS (i) at the onset; (ii) when the lowest (most severe) values were detected 2.4±1.5 months after onset (nadir); and (iii) 23.4±7.6 months after the onset as follow-up. Addenbrooke's Cognitive Examination test (ACE) was employed 23.4±7.6 months after onset of LGI1 LE [15]. Mental recovery score was calculated as the difference between the lowest MMSE score and the MMSE score at 23.4±7.6 months, and functional recovery score as the difference between the lowest mRS score and the mRS at 23.4±7.6 months. The study procedures were approved in Hungary and Denmark by the national ethics committees (082403/2015/OTIG and S-20140018). Written informed consents were obtained.

2.2 Magnetic resonance imaging

The initial MRI examinations were performed as part of the diagnostic procedures within one month after first occurence of the symptoms, and included axial- and coronal T_2-weighted Turbo Spin Echo (TSE), axial- and coronal Fluid-Attenuated Inversion Recovery (FLAIR), sagittal T_1-weighted TSE, three-dimensional T_1-weighted Magnetization Prepared Rapid Gradient Echo (MPRAGE) and single-shot diffusion weighted spin-echo echo planar imaging.

A prospective multi-modal MRI investigation was performed 33.1±18 months after the disease onset at two neuroimaging sites applying identical scanning protocols. Danish patients were scanned using a Siemens Magnetom® Verio™ 3T MR scanner and a 32-channel head coil

ACCEPTED MANUSCRIPT

(Siemens, Erlangen, Germany). Hungarian patients were scanned using a Siemens Magnetom® Trio™ and a 12-channel head coil. Both MR scanners were equipped with equivalent gradient systems (45mT/m @ 200T/m/s) and identical software versions (syngo® MR-B17). Scanning protocol consisted of a three-dimensional T_1-weighted 1 mm^3 isotropic MPRAGE sequence, axial, oblique axial and oblique coronal two-dimensional T_2-weighted TSE sequences, a two-dimensional FLAIR sequence, a two-dimensional single-shot diffusion weighted spin-echo Echo Planar Imaging sequence for Diffusion Tensor Imaging (DTI) and 1D PRESS sequence for single voxel ^1H spectroscopy (MRS) with one voxel placed in the right centrum semiovale (WM voxel) and another in the mid-occipital gray matter (GM voxel). Further details on the applied sequences are listed in the *Supplementary Materials and Methods*.

2.3 Data processing

2.3.1 Visual evaluation of acute phase and follow-up MRI

The structural MR images acquired in the subacute stage and at follow-up were compared with respect to edema and T2/FLAIR hyperintensity of the hippocampus. Evaluation of hippocampal sclerosis (increased T2 signal, reduced volume and/or abnormal morphology) was done on coronal plane images at the level of the hippocampus (or axial plane if coronal images were absent) [16].

2.3.2 Volumetric analysis of the T1-weighted MRI data

The partial volume corrected output volumes of caudate nucleus, putamen, pallidum, brain stem, hippocampus, amygdala, accumbens region, corpus callosum, cerebellar gray and white matter, as well as total cortical white matter and total segmented brain were calculated from automated volumetric analysis and were fed to further analyses [17,18]. Details of volumetric analysis method are described in the *Supplementary Materials and Methods*.

2.3.3 Diffusion tensor imaging and Tract-Based Spatial Statistics (TBSS)

Voxel-wise statistics were performed on the skeletonized data as described in the "*Statistical analysis*" section. For further analyses, mean skeletal FA and MD values were extracted form TBSS analysis pipeline and binary masks were generated for FA and MD from the voxels where

ACCEPTED MANUSCRIPT

FA or MD was significantly different between patients and controls [19-22]. Evaluation details are described in *Supplementary Materials and Methods*.

2.3.4 MR Spectroscopy evaluation

The CSF corrected concentration of the following metabolites were calculated in all MRS voxels [23-25]: total N-acetylaspartate (tNAA), total choline (tCho), total creatine (tCr), myo-inositole (Ins) and glutamine/glutamate (Glx). Detailed evaluation is described in *Supplementary Materials and Methods*.

2.4 Statistical analyses

For TBSS analysis, the voxelwise statistics were performed on the skeletonized data using a permutation-based non-parametric analysis [26]. Results were considered significant for $p<0.05$, corrected for multiple comparisons using threshold-free cluster enhancement [27], and all reported p-values of TBSS analyses are corrected p-values.

All other statistical analyses were performed using SPSS 20.0 (IBM Corp., Armonk, NY). For volumetric analysis, between-group comparisons employed multiple linear regression models with the volumes of the segmented brain structures as dependent variable and group membership (patient/control), age and total intracranial volume as independent variables. The same statistical approach was used to test for differences between patients and control subjects regarding brain metabolite concentration in GM and WM using the CSF corrected concentrations of metabolites as dependent variable, while age and group membership as independent variables. The assumptions of multiple linear regression were satisfied, as judged by testing for linearity, normality assumptions of the residuals, outliers, independence of errors, homoscedasticity and multi-collinearity. Correlation between clinical features measured on a continuous scale (mRS, MMSE and ACE) and the volumes of the segmented structures or the CSF corrected concentration of brain metabolite were assessed by partial correlations controlling for age and total intracranial volume or age respectively. To keep the number of statistical comparisons as low as possible for the comparisons with clinical features, only the onset and recovery values were used for mRS and MMSE, along with the ACE score measured at 23.4±7.6 months. Significance level was set at $p<0.05$, for multiple comparisons correction Benjamini–Hochberg procedure was applied with $q=10\%$. Results of statistical analyses performed with SPSS are

ACCEPTED MANUSCRIPT

reported with uncorrected p-values. However p-values that survive correction for multiple comparisons are always clearly marked.

ACCEPTED MANUSCRIPT

ACCEPTED MANUSCRIPT

3. RESULTS

3.1 Clinical data

All patients had limbic encephalitis. Although one Danish patient did not have manifest epilepsy, there were epileptic discharges in the left temporal lobe beside FBDS and dementia, and the patient received antiepileptic treatment (**Table 1**). Five patients had FBDS. No patient had status epilepticus. All patients received antiepileptic treatment. Seven patients received immunotherapy in the acute stage, which always included corticosteroids. Five patients received additional plasmapheresis, and one patient was treated with intravenous immunoglobulin. Immunosuppressive agents were orally administered over 15.2±8.0 months (**Table 1**). Cognitive abilities measured by MMSE at 24 months (median 27; range: 21-30) showed a five points improvement compared to nadir at 2.4±1.5 months (median 22; range: 10-28). The functional status evaluated by mRS at 23.4±7.6 months (median 2; range: 0-3) displayed a two points improvement compared to nadir (median 4; range: 3-5). Five patients showed cognitive decline at 24 months tested by ACE.

3.2 MRI findings in the acute stage

Diagnostic MRI scans were taken within one month after disease onset in eight patients **(Table 2)**. FLAIR images revealed unilateral (n=5) or bilateral (n=3) hyperintensities in the hippocampus in all eight patients. Seven of the eight patients showed unilateral (n=5) or bilateral (n=2) hyperintense signal changes in the hippocampus on T2-weighted images, whereas enhancing hippocampal lesions were only seen in one out of four patients on contrast-enhanced T1-weighted images.

Seven out of eight patients showed edema in the hippocampus as revealed by FLAIR and diffusion-weighted imaging (DWI) (bilateral n=2) (**Table 2**). Five patients displayed edema in the amygdala (bilateral n=2) and the temporal cortex was affected in two cases (unilateral; temporopolar and temporomesial).

None of the patients had extratemporal lesions.

3.3 Comparison of early and follow-up MRI findings

ACCEPTED MANUSCRIPT

MRI data obtained in the subacute stage were compared with those prospectively acquired 33.1±18 months after disease onset (**Table 2**). The number of patients identified with edema in the hippocampus decreased from 7 to 3 patients: remained unchanged in two, and appeared in one patient. Additional edema of the temporal cortex and amygdala on the FLAIR and diffusion-weighted scans was present on one case. In contrast, hippocampal T2 hyperintensity persisted in 6 patients (unilateral n=5, bilateral n=1) and FLAIR hyperintensity in seven cases (unilateral n=4, bilateral n=3). The extension of the T2/FLAIR hyperintensities decreased in one patient and remained constant in the other cases. The frequency of DWI/ADC alteration did not change (67%).

Eight of nine patients developed hippocampal sclerosis (unilateral=5, bilateral=3). All 8 patients diagnosed in the acute stage with seizures originating from the temporal lobe developed hippocampal sclerosis, although the site of epileptic focus and hippocampal sclerosis did not correlate. All patients were seizure free at time point of the follow up MRI.

3.4 Volumetric changes 33.1±18 months after disease onset

The mean volumes (±SD) of the segmented structures, based on the follow-up MRIs, are summarized in **Supplementary Table 1**. The total segmented brain volume was significantly lower in patients. Patients had significantly smaller volume in several brain areas (**Table 3**).

Next, we correlated the segmented brain structure volumes with the clinical features (mRS, MMSE and ACE). For such correlation, we used (i) midline structures with significant group differences (brainstem, combined volume of the mid-posterior and central parts of the corpus callosum); (ii) the bilateral volumes of those structures where significant difference were shown between patients and controls for both sides (cerebral white matter, cerebellar gray matter); (iii) and the bilateral volumes of lateral ventricles (a general marker of global atrophy) along with putamen and caudate, i.e. areas that have been shown to be highly affected by the disease [7-10]. Lower mRS score (better function) at onset was associated with higher cerebellar grey matter volume ($p=0.002$ $r=-0.932$, passing FDR correction) (**Figure 1**). Higher ACE test score (better cognition) at 23.4±7.6 months was associated with higher putaminal volume ($p=0.004$ $r=0.911$, passing FDR correction) (**Figure 1**). We observed additional trends related to mental and functional recovery (calculated as the difference between the lowest MMSE score and the MMSE score at 23.4±7.6 months, and the difference between the lowest mRS and the mRS at 23.4±7.6

ACCEPTED MANUSCRIPT

months), which did not remain significant after correction for multiple comparisons: higher putaminal volume and smaller dilation (volume) of the lateral ventricles was associated with better mental recovery ((p=0.025 r=0.816; and p=0.024, r=-0.819) (**Table 4**); better functional recovery was associated with higher volume of the central parts of the corpus callosum (p=0.04, r=0.777) (**Table 4**).

3.5 Widespread changes in white-matter microstructure 33.1±18 months after disease onset

Both fractional anisotropy (FA) and mean diffusivity (MD) analysis showed widespread reductions in patients ($p<0.05$) across the cerebellar and cerebral white matter (**Supplementary Table 2, Supplementary Table 3, Figure 2).** The average FA value (mean±SD) calculated from the entire FA skeleton was 0.40±0.01 for the healthy control subjects and 0.37±0.02 for the LGI1 patients. The mean MD value (mean±SD) was $0.83\pm0.03*10^{-3}mm^2*s^{-1}$ and $0.86\pm0.03*10^{-3}mm^2*s^{-1}$ respectively. Linear regression analyses controlled for age showed significant group differences for both average FA and average MD values ($p<0.001$ t=-5.445 and p=0.03 t=2.557).

3.6 Metabolic changes in the white and grey matter 33.1±18 months after disease onset

In the WM voxel, the CSF-corrected glutamine/glutamate concentrations were reduced in the patient group (p=0.019, t=-2.627 after correcting for multiple comparisons) **(Figure 3)**. There was a trend of reduction in the CSF-corrected choline concentrations (p=0.043, t=-2.210), but this was not significant after the FDR correction **(Figure 3)**. A trend of lower glutamine/glutamate concentration was found in the GM voxel (p=0.03, t=-2.445, non-significant after correcting for multiple comparisons) **(Figure 3)**. Both higher MMSE recovery score and higher ACE test scores at 24 months were associated with lower CSF corrected glutamine/glutamate concentrations measured in the WM voxel (p=0.013 r=-0.820 and p=0.008 r=-0.847), but neither survived correction for multiple comparisons.

ACCEPTED MANUSCRIPT

4. DISCUSSION

In this study, (i) we examined MRI alterations within one month after the onset of LGI1 encephalitis; (ii) used a prospectively planned multi-modal MRI to evaluate MRI outcomes 33.1±18 months after disease onset; and (iii) correlated MRI data with clinical outcomes at different time points during the course of the disease.

The most characteristic alterations in the acute LE phase were edema and T2/FLAIR hyperintensity of the hippocampus typical of LE [11,28,29]. We did not find extratemporal lesions, i.e. basal ganglia hyperintensities in our patients including FBDS cases in contrast to earlier studies [9,10,14,30,31]. Nevertheless, we found that higher volume of the putamen was associated with better cognition measured by ACE test at 23.4±7.6 months indicating the affection of the basal ganglia also in our studies, and that basal ganglia atrophy may affect functional outcomes in patients with LGI1 encephalitis. A very recent study also found that a longer duration of FBDS correlated with reduction of pallidum volume [14]. FLAIR hyperintensity of the hippocampus in the subacute stage was always followed by hippocampus atrophy on the same side, while T2 hyperintensity did not show such association. Presence of edema despite of clinical remission and seizure free condition may indicate persistent inflammation, but earlier epilepsy could also contribute: all 8 patients with manifest epilepsy at onset developed hippocampal sclerosis despite of absent seizure activity on follow-up.

Follow-up volumetry showed a significant volume decrease in the total segmented brain volume, white matter, corpus callosum, hippocampus, n. accumbens, brainstem and cerebellum. This may indicate that antibodies contribute to global tissue damage, or injury of the limbic structures induces secondary changes in other areas. The expression pattern of LGI1 with prominent staining in the hippocampus, the neocortex, thalamic nuclei and cerebellum corresponds to this observed atrophy, which may suggest a direct damage [32].

FA analysis also indicated diffuse deterioration of cerebral and cerebellar white matter integrity. Despite the lack of extratemporal lesions on conventional MRI during the acute stage, the most significant changes were measured in the anterior corona radiata, the anterior half of the capsula interna and the anterior 1/3 of the corpus callosum. The affection of frontal areas have been described in individual cases with VGKC encephalitis, although some of these patients did not have LGI1-antibodies [33,34].

ACCEPTED MANUSCRIPT

We found lower glutamine/glutamate concentrations in the WM compared to controls. A trend of lower concentration was seen in the GM voxel, but significance was lost after correcting for multiple comparisons. Since decreased glutamine/glutamate ratios were similarly observed in patients with depression and mood disorders [35,36], this may suggest the need for increased vigilance for affective disturbances in patients following LGI1 encephalitis. Considering structural MRI data indicating global atrophy, we expected a significant tNAA difference between the LGI1 patients and control subjects. Although the mean tNAA was somewhat lower in LGI1 group in both gray- and white matter, the difference was not significant. Since the mean age of the patients was around 60 years, it is possible that decrease of tNAA due to aging masks loss of tNAA related to the pathological condition.

We also correlated MRI outcomes with clinical data at onset, when the lowest (most severe) values were detected 2.4±1.5 months after onset (nadir), and after 23.4±7.6 months. Better functional outcome (mRS) at onset was associated with higher volume of the cerebellar gray matter. Such correlation in LGI1 encephalitis has not been described, but visually assessed irreversible cerebellar atrophy was associated with poor outcome in a recent study of NMDAR-encephalitis [37]. Better cognitive capacities measured by the ACE test at 23.4±7.6 months were also associated with higher putaminal volumes. The putamen is actively involved in a variety of cognitive functions such as episodic memory, cognitive control and category learning [38], and its inter-connection with frontal areas and hippocampus play an important role in cognition [39,40]. Hyperintensities previously published in VGKC and LGI1 encephalitis/FBDS pointed to the affection of these structures, and a very recent study reported correlation between longer duration of FBDS and pallidum volume [9,14,28-30]. Although we found decreased hippocampal volumes compared to matched controls, hippocampal volumetry did not correlate with ACE and mRS outcomes. In a very recent study, larger verbal memory deficits correlated with decreased volumes of the left hippocampus and its microstructural integrity [14].

In conclusion, our results indicate development of global brain atrophy in patients with LGI1 LE, despite of early immunotherapy. Besides alterations in the temporal limbic structures, we emphasize progressive alterations in the frontal lobe and the cerebellum. These changes may contribute to persistent cognitive dysfunction. Metabolic changes detected with MR spectroscopy indicate neuroinflammation and abnormal glutamine and glutamate levels. These results argue for the need of early, immediate treatment of LGI1 encephalitis. The benefit of patients treated as

ACCEPTED MANUSCRIPT

early as possible with first orwith second line immunotherapy if necessary is proven by several studies [41,42].

Our study is not without limitations. Only 9 patients and 9 control subjects were prospectively examined by multimodal MRI in two MR centers, and this may reduce the reliability of the applied statistical methods. The number of subjects per variable required for linear regression analyses is always subject of intensive debate, rules of thumb are usually between 5-10 subjects per variable. Although a recent study showed that adjusted R can be considered reliable at as low as 2 subjects per variable in certain cases [43], we tried to keep the numbers as low as possible (2 variables per 9 subjects or 3 variables per 18 subjects) for linear regression analyses. Since MRI in the acute stage of LE was acquired in different institutes using different protocols, the analyses of those sequences were limited. As the result of these limitations, further studies are required with larger cohorts to confirm our results and conclusions.

5. FUNDING

This work was supported by grants from Odense University Hospital and the University of Southern Denmark (to ZI). GO was supported by grants of the Janos Bolyai Research Scholarship of the Hungarian Academy of Sciences; and University of Pécs Medical School Research Fund (KA-2017-06).

6. SUPPLEMENTARY MATERIALS AND METHODS

1. **Sequence parameters:**

1.1 T_1-weighted MPRAGE sequence with an isotropic resolution of 1 mm to obtain anatomical images for MR-based volumetry and registration purposes (TR/TI/TE=2530/1100/3.37ms; Flip angle=7°; receiver bandwidth=200Hz/pixel; 176 contiguous sagittal slices; matrix size=256x256).

1.2 Two-dimensional T2-weighted turbo spin-echo (TSE) sequences: axial (TR/TE = 6000/78ms; Flip angle = 120°; receiver bandwidth = 220 Hz/pixel; 43 slices; 0.4mm gap, resolution = 0.7 x 0.7 x 4 mm^3); oblique axial (TR/TE = 3000/96ms; Flip angle = 120°; receiver bandwidth = 220 Hz/pixel; 17 slices; 1.2mm gap, resolution = 0.8 x 0.8 x 4 mm^3); oblique coronal (TR/TE = 3000/96ms; Flip angle = 120°; receiver bandwidth = 220

ACCEPTED MANUSCRIPT

Hz/pixel; 17 slices; 1.2mm gap, resolution = 0.7 x 0.7 x 4 mm^3). Oblique slices were perpendicular and parallel to the long axis of the hippocampus.

1.3 FLAIR sequence (TR/TE/TI=5000/95/1800ms; Flip angle=130°; receiver bandwidth=287Hz/pixel; 34 slices; 1.2mm gap, resolution=0.9x0.9x4mm^3) with oblique coronal slice orientation

1.4 MRS was performed using 1D PRESS sequence (TR/TE=2000/30ms; Flip angle=90°; chess water suppression; vector size=1024; delta frequency=-2.7ppm; bandwidth=1200Hz; averages=80). Voxel dimensions of white matter (WM) acquisitions were 15x15x15mm^3, while gray matter (GM) voxels measured 20x15x20mm^3. After automatic iterative shimming, manual shimming was performed to reduce the FWHM of the unsuppressed water signal as much as possible (inclusion criteria were <25Hz for GM and <20Hz for WM voxel). A fast reference water signal measurement was performed after each voxel with identical sequence properties and shim, except for no water suppression applied.

1.5 DTI images were acquired using a two-dimensional single-shot diffusion weighted spin-echo Echo Planar Imaging sequence (TR/TE=10100/91ms; 70 axial slices; slice thickness=2mm; no gap; FOV=208x256mm2; matrix size=128x128; bandwidth=1562Hz/pixel; EPI factor=104). Diffusion gradients were applied in 30 directions with a b-value of 900 s/mm2 and a single volume was collected with no diffusion gradients applied.

2. Volumetric analysis of the T1-weigted MR data:

MPRAGE images, acquired according to the Freesurfer's Morphometry Protocols Guideline, were fed into volumetric segmentation performed with FreeSurfer v5.3. Details of the procedures are described in previous publications [17,18]. Each dataset was checked within the processing stream to verify the Talairach transform, the accuracy of the skull strip, white matter- and pial surface segmentation, as described in the Recommended Reconstruction Workflow.

3. Diffusion tensor imaging and Tract-Based Spatial Statistics (TBSS) evaluation:

ACCEPTED MANUSCRIPT

Diffusion-weighted images were corrected for eddy current distortion and head motion using affine registration to a reference volume (B0). After brain extraction of the diffusion data using BET [19], FMRIB's diffusion toolbox was used to generate voxel-wise images of fractional anisotropy (FA) and mean diffusivity (MD) by fitting a diffusion tensor model to the data at each voxel of the brain [20]. Voxel-wise statistical analyses of FA and MD data were performed using TBSS v1.2 part of FMRIB's Software Library (FSL) [21]. First, all subjects' FA data were nonlinearly aligned to FMRIB58_FA standard space image using FNIRT [22]. Next, the mean FA image was thinned to generate a mean FA skeleton, which represents only the center of the white matter tracts common to all examined subjects. This mean skeleton was thresholded at FA>0.2.

4. MR spectroscopy evaluation:

Tissue type segmentation (GM, WM and CSF) of T1-weighted MPRAGE was performed using the FAST software implemented in FSL [23]. The binary masks of the MRS voxels were constructed in the native coordinate space of the MPRAGE image using Gannet software suite [24]. Average CSF content of the spectroscopy voxel was then calculated using the CSF image resulting from FAST and the binary mask of the voxel using fslstats. Spectroscopy data was evaluated using Tarquin (v4.3.6) with the following parameters: TE_1=10.8ms; Dynamic corr. ref. signals: ^{1}H, NAA, Cr, Cho, Lip; Water cutoff=45 Hz; Reference signals: ^{1}H, NAA, Cr, Cho, Lip; Auto phase; Auto reference; Eddy Current Correction; Internal basis set=^{1}H Brain + Glth; Water concentration=35880mM for WM and 43300mM for GM voxels; water attenuation=0.7; λ=0.2; Initial μ=0.001 [24]. As normalized fractions within the MRS voxel can be described as $f_{WM}+f_{GM}+f_{CSF}=1$, the CSF corrected metabolite concentration was calculated as $C = C_0 \times 1/(1-f_{CSF})$, where C_0 is the uncorrected metabolite concentration, and f_{CSF} is the average CSF fraction within the MRS voxel.

ACCEPTED MANUSCRIPT

7. DISCLOSURE OF CONFLICT OF INTEREST:

Dr. Illes reports grants from Biogen Idec, personal fees from Biogen Idec, personal fees from Sanofi Aventis/Genzyme, personal fees from Novartis, personal fees from Teva, outside the submitted work.

Dr. Siebner reports personal fees from Elsevier Publishers, Amsterdam, The Netherlands , personal fees from Springer Publishing, Stuttgart, Germany , grants and personal fees from Biogen Idec, Denmark A/S , personal fees from Genzyme, Denmark , and other from MagVenture, Denmark. All fees are outside the submitted work.

Dr. Garde reports personal fees from Biogen Idec, Denmark A/S, outside the submitted work.

Dr. Szots, Blaabjerg, Orsi, Iversene, Kondziella, Madsen, Magnusson, Barsi, and Nagy have nothing to disclose.

ACCEPTED MANUSCRIPT

ACCEPTED MANUSCRIPT

6. REFERENCES

1. Irani SR, Vincent A. Voltage-gated potassium channel-complex autoimmunity and associated clinical syndromes. Handb Clin Neurol 2016; 133: 185–197.

2. Malter MP, Frisch C, Schoene-Bake JC, Helmstaedter C, Wandinger KP, Stoecker W, et al. Outcome of limbic encephalitis with VGKC-complex antibodies: relation to antigenic specificity. J Neurol 2014; 261: 1695–1705.

3. Szots M, Marton A, Kover F, Kiss T, Berki T, Nagy F, et al. Natural course of LGI1 encephalitis: 3-5 years of follow-up without immunotherapy. J Neurol Sci 2014; 343: 198–202.

4. Ariño H, Armangué T, Petit-Pedrol M, Sabater L, Martinez-Hernandez E, Hara M, et al. Anti-LGI1-associated cognitive impairment: Presentation and long-term outcome. Neurology 2016; 87: 759–765.

5. van Sonderen A, Thijs RD, Coenders EC, Jiskoot LC, Sanchez E, de Bruijn MA, et al. Anti-LGI1 encephalitis: Clinical syndrome and long-term follow-up. Neurology 2016; 87: 1449–1456.

6. Irani SR, Stagg CJ, Schott JM, Rosenthal CR, Schneider SA, Pettingill P, et al. Faciobrachial dystonic seizures: the influence of immunotherapy on seizure control and prevention of cognitive impairment in a broadening phenotype. Brain 2013; 136: 3151–3162.

7. Plantone D, Renna R, Grossi D, Plantone F, Iorio R. Teaching NeuroImages: Basal ganglia involvement in facio-brachial dystonic seizures associated with LGI1 antibodies. Neurology 2013; 80: 183–184.

8. Boesebeck F, Schwarz O, Dohmen B, Graef U, Vestring T, Kramme C, et al. Faciobrachial dystonic seizures arise from cortico-subcortical abnormal brain areas. J Neurol 2013; 260: 1684–1686.

9. Flanagan EP, Kotsenas AL, Britton JW, McKeon A, Watson RE, Klein CJ, et al. Basal ganglia T1 hyperintensity in LGI1-autoantibody faciobrachial dystonic seizures. Neurol Neuroimmunol Neuroinflamm 2015; 2; e161.

10. Varley JA, Irani SR. Treating seizures and preventing amnesia in LGI1-antibody encephalitis: A new MRI signature? Neurol Neuroimmunol Neuroinflamm 2015; 2: e182.

11. Irani SR, Michell AW, Lang B, Pettingill P, Waters P, Johnson MR, et al. Faciobrachial dystonic seizures precede Lgi1 antibody limbic encephalitis. Ann Neurol 2011; 69: 892–900.

ACCEPTED MANUSCRIPT

12. Fidzinski P, Jarius S, Gaebler C, Boegner F, Nohr R, Ruprecht K. Faciobrachial dystonic seizures and antibodies to Lgi1 in a 92-year-old patient: A case report. J Neurol Sci 2014; 347: 404–405.

13. Wegner F, Wilke F, Raab P, Tayeb SB, Boeck AL, Haense C, et al. Anti-leucine rich glioma inactivated 1 protein and anti-N-methyl-D-aspartate receptor encephalitis show distinct patterns of brain glucose metabolism in 18F-fluoro-2-deoxy-d-glucose positron emission tomography. BMC Neurol 2014; 14: 136.

14. Finke C, Prüss H, Heine J, Reuter S, Kopp UA, Wegner F, et al. Evaluation of cognitive deficits and structural hippocampal damage in encephalitis with Leucine-rich, glioma-inactivated 1 antibodies. JAMA Neurology 2017; 74: 50–59.

15. Mioshi E, Dawson K, Mitchell J, Arnold R, Hodges JR. The Addenbrooke's cognitive examination revised (ACE-R): a brief cognitive test battery for dementia screening. Int J Geriatr Psychiatry 2006; 21: 1078–1085.

16. Bronen R. MR of mesial temporal sclerosis: how much is enough? Am J Neurorad 1998; 19: 15–18.

17. Fischl B, Salat DH, Busa E, Albert M, Dieterich M, Haselgrove C, et al. Whole brain segmentation: automated labeling of neuroanatomical structures in the human brain. Neuron 2002; 33: 341–355.

18. Fischl B, Salat DH, van der Kouwe AJ, Makris N, Ségonne F, Quinn BT, et al. Sequence-independent segmentation of magnetic resonance images. Neuroimage 2004; 23: 69–84.

19. Smith SM. Fast robust automated brain extraction. Human Brain Mapping 2002; 17: 143–155.

20. Smith SM, Jenkinson M, Woolrich MW, Beckmann CF, Behrens TE, Johansen-Berg H, et al. Advances in functional and structural MR image analysis and implementation as FSL. Neuroimage 2004; 23: 208–219.

21. Smith SM, Jenkinson M, Johansen-Berg H, Rueckert D, Nichols TE, Mackay CE, et al. Tract-based spatial statistics: voxelwise analysis of multi-subject diffusion data. Neuroimage 2006; 31: 1487–1505.

22. Andersson JLR, Jenkinson M, Smith SM. Non-linear registration, aka spatial normalisation. FMRIB technical report TR07JA2. 2007b.

ACCEPTED MANUSCRIPT

23. Zhang Y, Brady M, Smith S. Segmentation of brain MR images through a hidden Markov random field model and the expectation-maximization algorithm. IEEE Trans Med Imaging 2001; 20: 45–57.

24. Harris AD, Puts NA, Edden RA. Tissue correction for GABA-edited MRS: Considerations of voxel composition, tissue segmentation, and tissue relaxations. J Magn Reson Imaging 2015; 42: 1431–1440.

25. Wilson M, Reynolds G, Kauppinen RA, Arvanitis TN, Peet AC. A constrained least-squares approach to the automated quantitation of in vivo 1H magnetic resonance spectroscopy data. Magn Reson Med 2011; 65: 1–12.

26. Winkler AM, Ridgway GR, Webster MA, Smith SM, Nichols TE. Permutation inference for the general linear model. Neuroimage 2014; 92: 381–397.

27. Smith SM, Nichols TE. Threshold-free cluster enhancement: Addressing problems of smoothing, threshold dependence and localisation in cluster inference. Neuroimage 2009; 44: 83–98

28. Kotsenas AL, Watson RE, Pittock SJ, Britton JW, Hoye SL, Quek AM, et al. MRI findings in autoimmune voltage-gated potassium channel complex encephalitis with seizures: one potential etiology for mesial temporal sclerosis. Am J Neuroradiol 2014; 35: 84–89.

29. Urbach H, Soeder BM, Jeub M, Klockgether T, Meyer B, Bien CG. Serial MRI of limbic encephalitis. Neuroradiology 2006; 48: 380–386.

30. Shin YW, Lee ST, Shin JW, Moon J, Lim JA, Byun JI, et al. VGKC-complex/LGI1-antibody encephalitis: clinical manifestations and response to immunotherapy. J Neuroimmunol 2013; 265: 75–81.

31. Heine J, Prüss H, Bartsch T, Ploner CJ, Paul F, Finke C. Imaging of autoimmune encephalitis - Relevance for clinical practice and hippocampal function. Neuroscience 2015; 309: 68–83.

32. Schulte U, Thumfart JO, Klöcker N, Sailer CA, Bildl W, Biniossek M, et al. The epilepsy-linked Lgi1 protein assembles into presynaptic Kv1 channels and inhibits inactivation by Kvbeta1. Neuron 2006; 49: 697–706.

33. Newey CR, Appleby BS, Shook S, Sarwal W. Patient with voltage-gated potassium-channel (VGKC) limbic encephalitis found to have Creutzfeldt-Jakob disease (CJD) at autopsy. J Neuropsychiatry Clin Neuroscience 2013; 25: 5–7.

ACCEPTED MANUSCRIPT

34. McKeon A, Marnane M, O'Connell M, Stack JP, Kelly PJ, Lynch T. Potassium channel antibody–associated encephalopathy presenting with a frontotemporal dementia–like syndrome. Arch Neurology 2007; 64: 1528–1530.

35. Hasler G, van der Veen JW, Tumonis T, Meyers N, Shen J, Drevets WC. Reduced prefrontal glutamate/glutamine and gamma-aminobutyric acid levels in major depression determined using proton magnetic resonance spectroscopy. Arch Gen Psychiatry 2007; 64: 193–200.

36. Yüksel C, Öngür D. Magnetic Resonance Spectroscopy Studies of Glutamate-Related Abnormalities in Mood Disorders. Biol Psychiatry 2010; 68: 785–794.

37. Iizuka T, Kaneko J, Tominaga N, Someko H, Nakamura M, Ishima D,et al. Association of progressive cerebellar atrophy with long-term outcome in patients with anti-N-methyl-D-aspartate receptor encephalitis. JAMA Neurology 2016; 73: 706–713.

38. Ell SW, Helie S, Hutchinson S. Contributions of the Putamen to Cognitive Function. In: Costa A, Villalba E, eds. Horizons in neuroscience research. Hauppauge NY: Nova science publishers, 2012: 29–52.

39. van Schouwenburg MR, O'Shea J, Mars RB, Rushworth MF, Cools R. Controlling human striatal cognitive function via the frontal cortex. J Neurosci 2012; 32: 5631–5637.

40. Seger CA, Dennison CS, Lopez-Paniagua D, Peterson EJ, Roark AA. Dissociating hippocampal and basal ganglia contributions to category learning using stimulus novelty and subjective judgments. Neuroimage 2011; 55: 1739–1753.

41. Ismail FS, Popkirov S, Wellmer J, Grönheit W. Faciobrachio-crural dystonic seizures in LGI1 limbic encephalitis: A treatable cause of falls. Neurol Neuroimmunol Neuroinflamm 2015; 2: e146.

42. Dogan Onugoren M, Golombeck KS, Bien C, Abu-Tair M, Brand M, Bulla-Hellwig M, et al. Immunoadsorption therapy in autoimmune encephalitides. Neurol Neuroimmunol Neuroinflamm 2016; 3: e207.

43. Austin PC, Steyerberg EW. The number of subjects per variable required in linear regression analyses. J Clin Epidemiol 2015; 68: 627–636.

ACCEPTED MANUSCRIPT

LEGENDS

Figure 1 Correlation of cerebellar grey matter and putaminal volume with functional outcomes

Plots A and B were created using demeaned data, where 0 represents the mean value on both axes. **A.** Partial regression plot demonstrating the significant negative relationship between total cerebellar grey matter volume and mRS test score at onset after the effects of intracranial volume and age was removed. **B.** Partial regression plots demonstrating the significant positive relationships between putaminal volume and ACE test score at 24 months after the effects of intracranial volume and age was removed.

(R^2)=linear correlation coefficient, ACE=Addenbrook's Cognitive Examination, mRS=modified Rankin scale

Figure 2 Tract-based spatial statistics analysis of the white matter in patients with LGI1 limbic encephalitis

Red/yellow: significant differences (corrected $p<0.05$) in fractional anisotropy (FA) between patients (n=9) and controls (n=9). Blue/light blue: significant differences (corrected $p<0.05$) in mean diffusivity (MD) between patients and controls. Overlapping regions are marked green.

Figure 3 Single-voxel MR spectroscopy in patients with LGI1 limbic encephalitis

Mid-occipital white (**A**) and gray matter (**B**) spectroscopy. Horizontal line: median; +: mean; box: interquartile range (25–75%). The difference ($p=0.027$) in GM has not survived FDR correction. tNAA: total N-acetylaspartate; tCho: total choline; tCr: total creatine; Ins: myo-inositole; Glx: glutamine/glutamate

ACCEPTED MANUSCRIPT

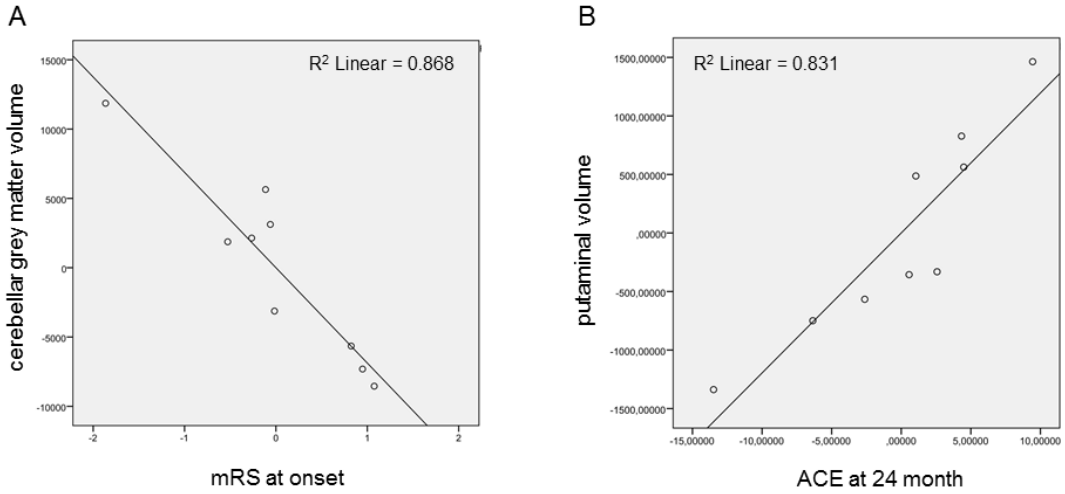

Fig. 1

ACCEPTED

ACCEPTED MANUSCRIPT

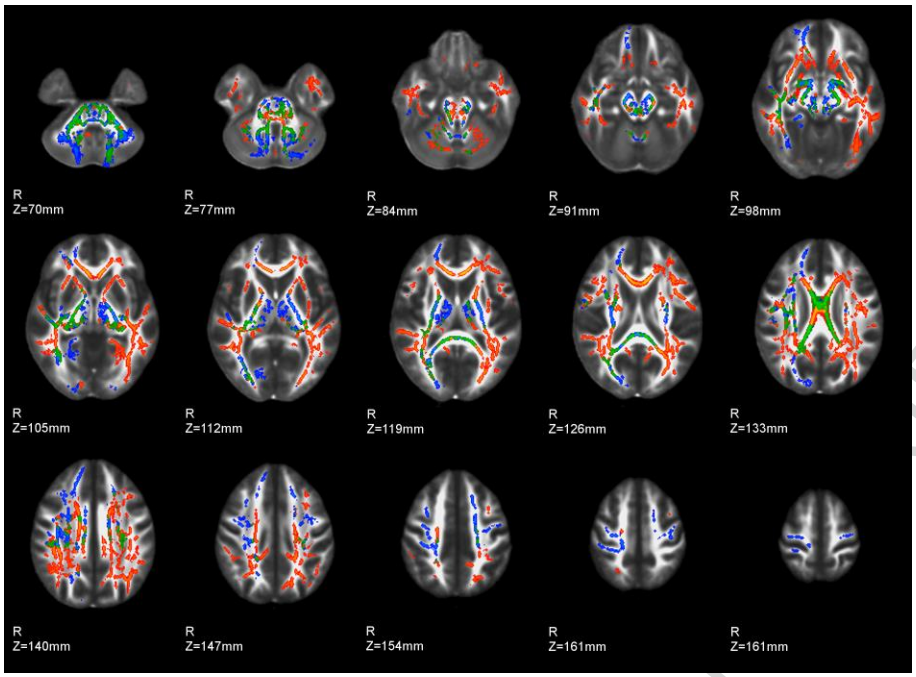

Fig. 2

ACCEPTED MANUSCRIPT

ACCEPTED MANUSCRIPT

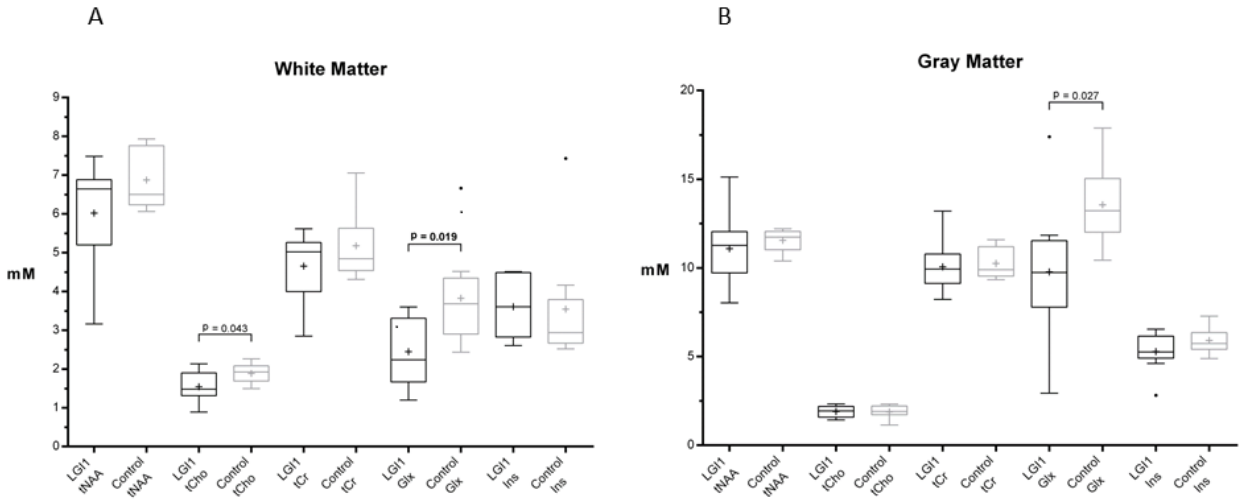

Fig. 3

ACCEPTED MANUSCRIPT

ACCEPTED MANUSCRIPT

Table 1 Clinical characteristics of the patients with LGI1 limbic encephalitis

Characteristics	Number of patients, mean and median values
Demographics	
Number of patients	9
Age at onset (mean±SD years)	59.9±14.5
Sex (male/female)	5/4
Symptoms (number of patients)	
Faciobrachial dystonic seizures	5
Epilepsy	8[a]
Temporal lobe epilepsy	8[a]
Epileptiform discharges on EEG	7
Status epilepticus	0
Memory impairment	
Mini-Mental State Examination score at onset (median)	25 (range: 21-30)
Mini-Mental State Examination score at nadir (median)	22 (range: 10-28)
Mini-Mental State Examination score at 24 months control (median)	27 (range: 21-30)
Addenbrooke test score <83 at 24 months control	5
Functional ability	
Modified Rankin scale at onset (median)	3 (range: 1-4)
Modified Rankin scale at nadir[b] (median)	4 (range: 3-5)
Modified Rankin scale at 24 months (median)	2 (range: 0-3)
Laboratory abnormalities (serum)	
Serum sodium level <136 mmol/L	8
LGI1 antibody	9
Other autoimmune antibodies	0
Therapy	
Start of immunotherapy (months from onset, mean±SD)	1.8±1.4
Duration of per os immunotherapy (months, mean±SD)	15.2±8.0
Administration of immunotherapy (number of patients)	7

ACCEPTED MANUSCRIPT

Steroids	7
Plasma exchange	5
Intravenous immunoglobulin	1
Other immunosuppressive agents (cyclophosphamide, azathioprine)	4
Antiepileptic drugs	9
Tumor	0

[a]Although one Danish patient did not have manifest epilepsy, there were epileptic discharges in the left temporal lobe beside FBDS and dementia, and the patient received antiepileptic treatment.

[b]2.4±1.5 months; reference ranges of laboratory results are given in parenthesis. SD: standard deviation; LGI1: Leucin-rich glioma-inactivated 1 protein; EEG: electroencephalography; CSF: cerebrospinal fluid

ACCEPTED MANUSCRIPT

ACCEPTED MANUSCRIPT

Table 2 Characteristics of acute and follow-up conventional MRI sequences by visual evaluation in patients with LGI1 limbic encephalitis

	MRI acute	**MRI follow-up**
Time from onset of the disease (months) (mean±SD)	≤1 month	33.11±17.97
Edema		
hippocampus	7/8 (88%)	3/9 (33%)
amygdala	5/8 (63%)	1/9 (11%)
temporal cortex	2/8 (26%)	1/9 (11%)
extratemporal	0/8 (0%)	0/9 (0%)
Hippocampus		
T2 hyperintensity	7/8 (88%)	6/9 (67%)
FLAIR hyperintensity	8/8 (100%)	7/9 (78%)
T1 contrast enhancement	1/4 (25%)	NA
DWI/ADC signal changes	4/6 (67%)	6/9 (67%)

Data are shown as number of patients/available data (percentage)

FLAIR: fluid-attenuated inversion recovery; DWI: diffusion-weighted imaging; ADC: apparent diffusion coefficient; NA: not applicable

ACCEPTED MANUSCRIPT

ACCEPTED MANUSCRIPT

Table 3 Significant differences in regional brain volumes on follow-up MRI between control subjects and patients with LGI1 limbic encephalitis

Segmented structure	p value	t value
Left Lateral Ventricle	0.115	1.681
Left Cerebellum White Matter	0.060	-2.047
Left Cerebellum Cortex	**0.031**	**-2.391**
Left Thalamus Proper	0.462	-0.756
Left Caudate	0.652	-0.460
Left Putamen	0.582	0.563
Left Pallidum	0.269	-1.151
Brain Stem	**<001**	**-4.524**
Left Hippocampus	0.421	-0.828
Left Amygdala	0.161	1.480
Left Accumbens area	**0.021**	**-2.589**
Right Lateral Ventricle	**0.006**	**3.210**
Right Cerebellum White Matter	**0.035**	**-2.330**
Right Cerebellum Cortex	**0.017**	**-2.703**
Right Thalamus Proper	0.049	-2.155
Right Caudate	0.487	-0.714
Right Putamen	0.923	0.097
Right Pallidum	0.481	-0.724
Right Hippocampus	**0.012**	**-2.869**
Right Amygdala	0.189	-1.380
Right Accumbens area	0.176	-1.424

ACCEPTED MANUSCRIPT

Corpus Callosum Posterior	0.761	-0.310
Corpus Callosum Mid Posterior	**0.020**	**-2.635**
Corpus Callosum Central	**0.021**	**-2.611**
Corpus Callosum Mid Anterior	0.153	-1.510
Corpus Callosum Anterior	0.328	-1.013
Segmented Brain volume	**0.023**	**-2.553**
Cortical volume, left hemisphere	0.298	1.081
Cortical volume, right hemisphere	0.869	0.167
White Matter volume, left hemisphere	**0.015**	**-2.769**
White Matter volume, right hemisphere	**0.009**	**-3.048**

Positive t value means larger structure volume in patients. Corrected for age and total intracranial volume. P values in bold survive Benjamini–Hochberg procedure for multiple comparison correction with q = 10%.

ACCEPTED MANUSCRIPT

ACCEPTED MANUSCRIPT

Table 4 Significant correlations between clinical features and the volumes of segmented structures in patients with LGI1 limbic encephalitis

		Cerebral WM	*Total cerebellar GM*	*CC MID + Central*	*Bilateral Ventricle*	*Brain-stem*	*Putamen*	*Caudate*
mRS onset	Correlation	-0.110	**-0.932**	-0.304	-0.235	-0.619	0.438	0.208
	Significance (2-tailed)	0.814	**0.002**	0.507	0.612	0.138	0.326	0.655
mRS recovery[a]	Correlation	0.729	0.550	0.777	-0.376	0.105	0.239	0.385
	Significance (2-tailed)	0.063	0.201	0.040	0.406	0.823	0.606	0.394
MMSE onset	Correlation	0.134	-0.446	-0.063	-0.739	-0.645	-0.057	-0.203
	Significance (2-tailed)	0.775	0.315	0.893	0.058	0.118	0.904	0.663
MMSE recovery[b]	Correlation	0.248	-0.402	0.064	-0.819	-0.597	0.816	0.014
	Significance (2-tailed)	0.591	0.371	0.892	0.024	0.157	0.025	0.976
ACE at 24 months	Correlation	0.134	-0.446	-0.063	-0.739	-0.645	**0.911**	0.168
	Significance (2-tailed)	0.775	0.315	0.893	0.058	0.118	**0.004**	0.719

Controlled for age and total intracranial volume. mRS: modified Rankin scale, ACE: Addenbrooke's Cognitive Examination, MMSE: Mini-Mental State Examination. [a]Difference between the lowest mRS score and the mRS score at 23.4±7.6 months, [b]Difference between the lowest MMSE score and the MMSE score at 23.4±7.6 months. WM: white matter, GM: gray

ACCEPTED MANUSCRIPT

matter, CC: corpus callosum, MID: mid-posterior. Significant correlations surviving FDR correction are in bold.

ACCEPTED MANUSCRIPT

ACCEPTED MANUSCRIPT

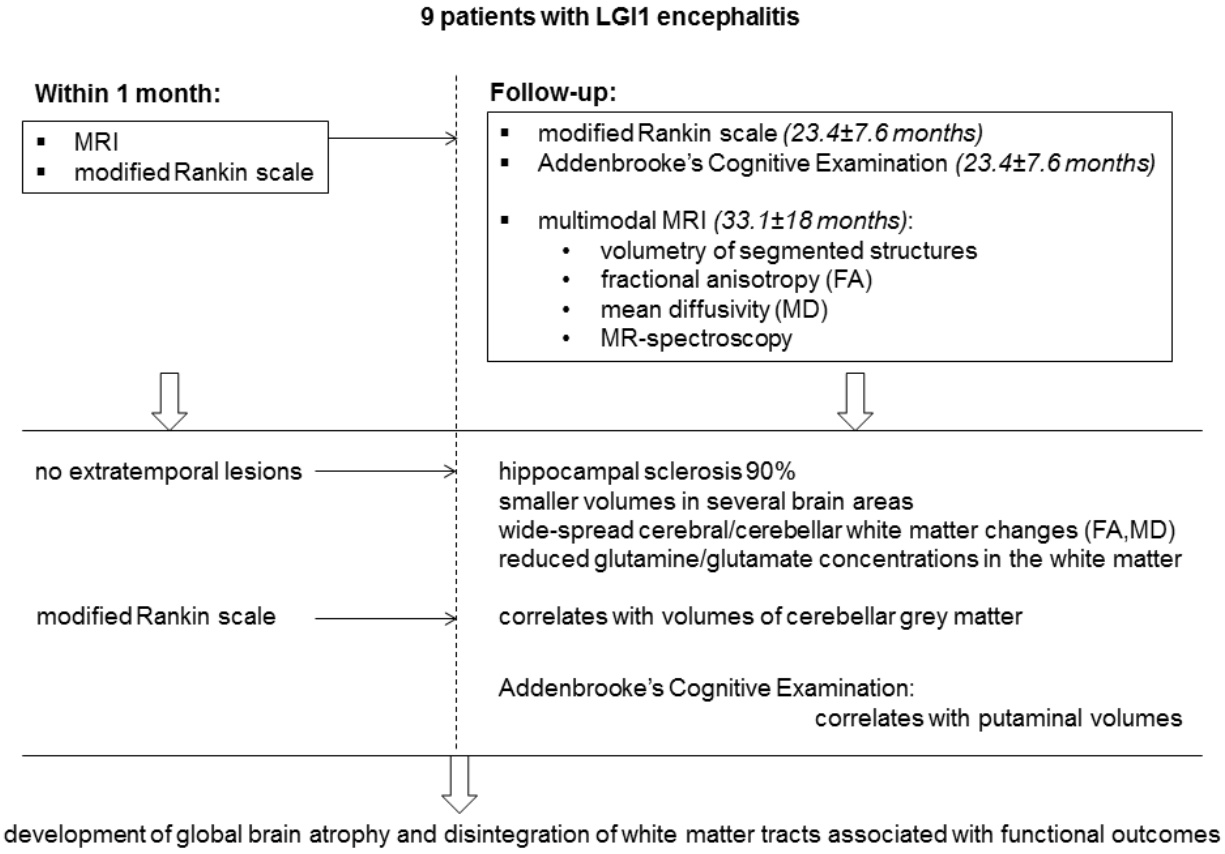

Graphical abstract

ACCEPTE

ACCEPTED MANUSCRIPT

Highlights

- Cerebral and cerebellar atrophy developed in 9 patients with LGI1 encephalitis.
- Modified Rankin score at onset correlated with volumes of the cerebellar grey matter.
- Addenbrooke's Cognitive Examination at follow-up correlated with putaminal volume.
- Fractional anisotropy and mean diffusivity showed wide-spread white matter changes.
- MR-spectroscopy showed reduced glutamine/glutamate concentration in the white matter.

ACCEPTED MANUSCRIPT